Study of spatial correlations between radiation-induced defects and the activator Eu^{2+} in the X-ray storage phosphor $BaFBr:Eu^{2+}$ with optical detection of electron paramagnetic resonance

1992 J. Phys.: Condens. Matter 4 8919

(http://iopscience.iop.org/0953-8984/4/45/024)

J. Phys.: Condens. Matter 4 (1992) 8919–8932. Printed in the UK

Study of spatial correlations between radiation-induced defects and the activator Eu^{2+} in the x-ray storage phosphor BaFBr:Eu^{2+} with optical detection of electron paramagnetic resonance

F K Koschnick†, J-M Spaeth† and R S Eachus‡

† University of Paderborn, Fachbereich Physik, Warburger Strasse 100, 4790 Paderborn, Federal Republic of Germany

‡ Research Laboratories, Eastman Kodak Company, Rochester, NY 14650–2021, USA

Received 10 August 1992

Abstract. For the understanding of the photostimulated emission process of the storage phosphor BaFBr it was assumed that a spatial correlation exists between the F centres and hole centres generated by x-rays and the activator ion Eu^{2+}. We present direct experimental evidence for such a correlation with the detection of cross-relaxation effects in the optically detected electron paramagnetic resonance. A quantitative analysis of the intensity and spectral shape of the Eu^{2+} cross-relaxation spectra is presented. It follows that a substantial fracture of F centres and O^- centres (in oxygen-containing BaFBr) are generated with a distance of about 20 Å from the Eu^{2+} activators.

1. Introduction

Europium-doped barium fluorobromide is an important x-ray phosphor material (Luckey 1975, Stevels *et al* 1975). During x-irradiation trapped electron and hole centres are formed. The electrons are trapped at two different sites: at fluoride vacancies to produce $F(F^-)$ and at bromide vacancies to produce $F(Br^-)$ centres (Koschnick *et al* 1992a). Hole centres were found to be $Br_2^- - V_K$ centres which are stable up to 120 K. They consist of a hole shared by two out-of-plane bromide ions (Eachus *et al* 1991a, Koschnick *et al* 1992b). Also oxygen impurity defects are formed which are located on fluorine sites (O_F^- centres) and which are room-temperature stable (Eachus *et al* 1991a,b, Koschnick *et al* 1992b).

The stored images are read out by optical stimulation into the F bands which leads to electron–hole recombinations and an emission of the activator ion Eu^{2+} at 3.19 eV (Brixner *et al* 1980). The fundamental mechanisms of the generation of the image storage centres and their recombination are not really understood. Especially, the nature of the hole centres which are taking part in the read out process (photostimulated luminescence (PSL)), is not clear in this stage of investigation. The role of the oxygen impurities in the PSL process is not yet fully understood. Another fundamental problem is that one must assume a spatial correlation between the radiation-produced electron and hole centres and the activator ions in order to understand the PSL effect considering the very low concentration of radiation-produced centres of the order of 10^{12} and 10^{13} cm^{-3} (von Seggern *et al* 1989)

0953-8984/92/458919+14$07.50

compared to the concentration of activator ions ($\approx 10^{18}$ cm^{-3}). A first experimental indication for a spatial correlation between F centres, hole centres and the activator Eu^{2+} was obtained by Hangleiter *et al* (1990). It was shown by temperature-dependent measurements of the PSL that PSL active complexes (so called 'triple' centres which consist of an F centre, a hole centre and the activator ion Eu^{2+}) must be formed under x-irradiation.

In this paper we report on cross-relaxations between the radiation-induced defects and the Eu^{2+} ions. We show that cross-relaxation effects between spatially correlated defects can be observed when optically detecting the electron paramagnetic resonance (ODEPR) using the absorption method (Ahlers *et al* 1983). For the first time a quantitative analysis of the cross-relaxation effects observed in ODEPR is presented from which important information on the spatial correlation between defects can be obtained. A first account of the major results was published by Koschnick *et al* (1991). In this paper a detailed account of this novel kind of cross-relaxation spectroscopy is presented.

2. Experimental procedure

Single crystals of BaFBr:Eu^{2+} were grown by the Bridgman Stockbarger method in graphite crucibles coated with pyrolytic graphite. Eu doping was performed by adding of EuF_2 to the components BaF_2 and $BaBr_2$ before crystal growth. The nominal doping level of Eu^{2+} was between 10 ppm and 100 ppm. x-irradiation at room temperature was performed with an x-ray tube (50 kV, 40 mA) with a distance of 10 cm between the anode and the sample. *In situ* x-irradiation at $T = 4.2$ K was performed with a tube at 60 kV and 15 mA.

Optically detected EPR was measured as microwave-induced changes of the magnetic circular dichroism of the absorption (MCDA) with a custom built, computer-controlled ODEPR spectrometer working in K band (24 GHz) and at 1.5 K (Ahlers *et al* 1983). The MCDA is the differential absorption of right and left circularly polarized light along a static magnetic field. It is proportional to the spin polarization of the ground state of a paramagnetic Kramers defect. The change in spin polarization by EPR transitions can be monitored as a change of the MCDA of a defect (Ahlers *et al* 1983).

3. Experimental results

Upon x-irradiation of europium-doped BaFBr (doping level below 100 ppm) the same radiation-induced centres are formed as in undoped BaFBr. In undoped BaFBr, without special oxygen removal treatment, both types of F centres, O_F^- centres, and after low temperature x-irradiation $Br_2^- - V_K$ centres are produced (see Eachus *et al* 1991a,b, Koschnick *et al* 1992a,b). Figure 1 shows the MCDA spectrum of BaFBr: Eu^{2+} (100 ppm) x-irradiated at room temperature. The MCDA bands of $F(Br^-)$, $F(F^-)$ and O_F^- centres are measured as well as MCDA transitions of Eu^{2+}. The spectral shapes of the MCDA spectra of the irradiation-induced F and O_F^- centres are not influenced by the Eu doping (doping level below 100 ppm). Optically detected electron nuclear double resonance (ODENDOR) experiments on $F(Br^-)$ centres showed that up to the fourth shell of neighbours no differences are found compared to $F(Br^-)$ centres in

undoped crystals. Further shells are not resolved in ODENDOR and the concentration of F centres is too low for conventional ENDOR measurements (Koschnick *et al* 1992). Thus, no $F(Br^-)$– Eu^{2+} close pairs are formed.

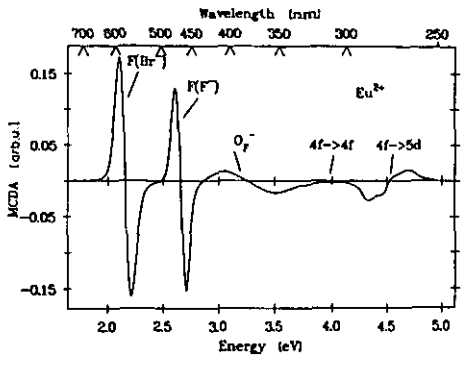

Figure 1. MCDA spectrum of europium-doped BaFBr after x-irradiation at room temperature measured at a temperature of 1.5 K and a magnetic field of 3 T parallel to the tetragonal c axis. The MCDA bands of the two types of F centres ($F(Br^-)$ and $F(F^-)$ centre), the oxygen hole centre (O_F^-) and the Eu^{2+} defect can be seen.

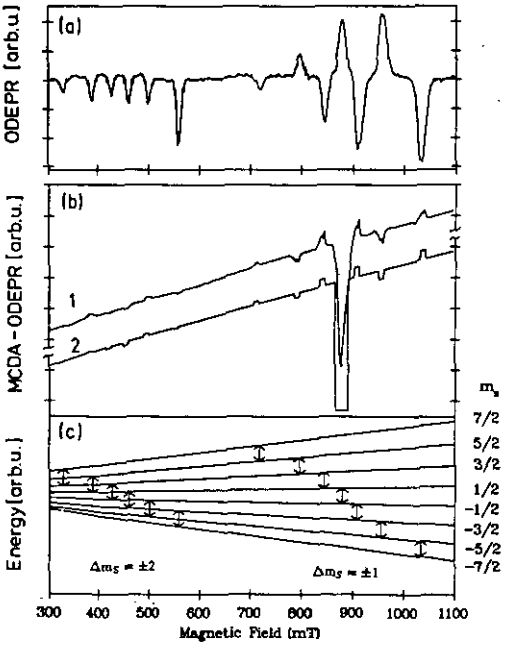

Figure 2. (a) ODEPR spectrum of Eu^{2+} measured in the Eu^{2+} 4f → 5d transition at 4.37 eV, T = 1.5 K, ν = 24 GHz, $\boldsymbol{B} \parallel c$-axis. (b) Curve 1: MCDA of $F(Br^-)$ centres at 2.1 eV and the microwave-induced ODEPR transitions showing the EPR spectrum of $F(Br^-)$ centres and cross-relaxation lines of Eu^{2+} in BaFBr:Eu doped with 50 ppm Eu^{2+}. T = 1.5 K, ν = 24 GHz, $\boldsymbol{B} \parallel c$-axis. Curve 2: Calculated cross-relaxation spectrum assuming R = 0.1 s^{-1} between $F(Br^-)$ centres in Eu^{2+} at a fixed distance. For simplicity the line shape was assumed to be rectangular (see text). (c) Breit–Rabi diagram for Eu^{2+} defects in BaFBr with EPR transitions at 24 GHz. The transition $\Delta m_S = \pm 1$ represents the 7 allowed fine structure lines, the low field transitions represent forbidden lines.

However, a significant influence of the presence of Eu^{2+} was found in the ODEPR spectra. Figure 2(b), curve 1, shows the ODEPR spectrum, measured in the MCDA of the $F(Br^-)$ centres of room temperature x-irradiated Eu-doped BaFBr (doping level ≈ 100 ppm). In addition to the F-centre resonance at about 885 mT, the lines of Eu^{2+} can be seen in the ODEPR spectrum. The line positions of the Eu^{2+} resonances are exactly in agreement with those measured directly in the Eu^{2+} MCDA (Koschnick *et al* 1992c) (see figure 2(a)). The remarkable change in sign of the

ODEPR lines of the Eu^{2+} is caused by forbidden spin–lattice relaxations, which connect Zeeman levels with $\Delta m_S = \pm 2$ faster than those with $\Delta m_S = \pm 1$. A quantitative explanation of this unusual sign change of ODEPR lines is given in Koschnick (1992c). In figure 2(a) the MCDA effect due to the spin polarization of the Eu^{2+} ground state described by a Brillouin function for $S = 7/2$ and the Eu^{2+} g-factor was subtracted, in figure 2(b), curve 1, the ODEPR lines are shown as microwave-induced deviations from the F-centre Brillouin function. The magnetization curve of the $F(Br^-)$, which is proportional to the MCDA, is identical to the curve one measures in undoped BaFBr. It is concluded that the spins of the $F(Br^-)$ centres are not coupled to the Eu^{2+} spins as to yield a total spin of $(7/2 \pm 1/2)$. This confirms the results from the ODENDOR measurements of $F(Br^-)$ centres that there is no direct proximity relationship between the $F(Br^-)$ centres and the Eu^{2+} ions. In such a case one would also expect a splitting of the ODEPR lines due to the spin–spin interaction between the $S = 1/2$ (F centre) and $S = 7/2$ (Eu^{2+}) spin systems. Assuming for such an interaction the classical point dipole–dipole interaction, then the distance between $F(Br^-)$ and Eu^{2+} must be larger than 15Å. For a smaller distance the splitting would have been resolved.

Therefore the Eu^{2+} lines in the ODEPR spectrum measured in the MCDA of the $F(Br^-)$ centre can only be caused by a relatively weak spin–spin interaction which produces a cross-relaxation between the two different spin systems. The cross-relaxation effect observed did not depend on the intensity of the measurement light. Therefore, cross-relaxation triggered by optical pumping can be ruled out (Geschwind 1972). The same Eu^{2+} resonances were also found in the ODEPR spectra measured in the MCDA of the $F(F^-)$ centres, the O_F^- centres and the Br_2^-–V_K centres (see figure 3). Also for those centres the separation from Eu^{2+} must exceed 15 Å.

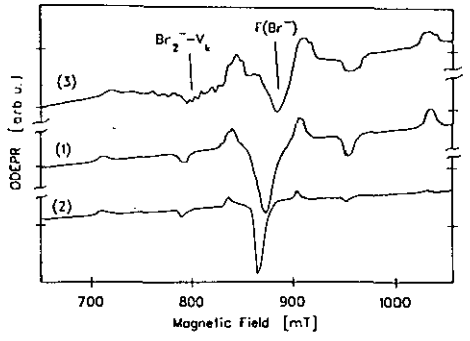

Figure 3. ODEPR spectra measured in the MCDA bands of the $F(F^-)$ centre (1), the O_F^- centre (2) and the Br_2^-–V_K centre (3) at $T = 1.5$ K and a microwave frequency of 24 GHz, $B \parallel c$. The spectra of the $F(F^-)$ centres (1) and the O_F^- centres (2) show cross-relaxations to the Eu^{2+} defects. The spectrum measured in the MCDA of the Br_2^-–V_K centres (3) shows cross-relaxations to the $F(Br^-)$ centres and to the Eu^{2+} defects.

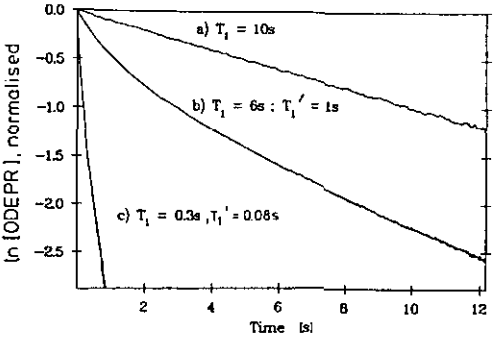

Figure 4. ODEPR decay curves of the $F(Br^-)$ EPR lines in a semilogarithmic plot, $T = 1.5$ K, $B = 880$ mT, x-irradiation at room temperature, for (a) undoped BaFBr, (b) BaFBr: 10 ppm Eu^{2+}, (c) BaFBr: 70 ppm Eu^{2+}. The decay curves were fitted with 2 exponentionals.

In order to further elucidate the mechanism of the cross-relaxation, time-resolved ODEPR measurements were performed. The T_1 times of the ODEPR lines were

measured for various Eu^{2+} concentrations. Measures were taken to ascertain that the concentration of the F centres was kept below $\approx 10^{16}$ cm^{-3} in order to prevent any interactions among the radiation defects. Figure 4 shows as an example the decay curve of the ODEPR effect of the $F(Br^-)$ centres measured at $T = 1.5$ K via the main ODEPR transition at 890 mT for various Eu^{2+} concentrations which were determined by atomic absorption. The vanishing of the ODEPR effect was monitored after switching off the microwaves as a function of time. Normally thermal equilibrium of the MCDA is reached exponentially with the spin–lattice relaxation time T_1. Without Eu^{2+} doping the $F(Br^-)$ centre has a spin–lattice relaxtion time of $T_1 = 10$ s. With increasing doping level T_1 decreases and the decay curve cannot be described by one single exponential any more. For a doping level of 100 ppm Eu^{2+} the spin–lattice relaxation of the F centres is almost the same as that of the Eu^{2+} defects. In this case, the coupling of the F-centre spins and the Eu^{2+} spins by cross-relaxation effects seems to be very efficient.

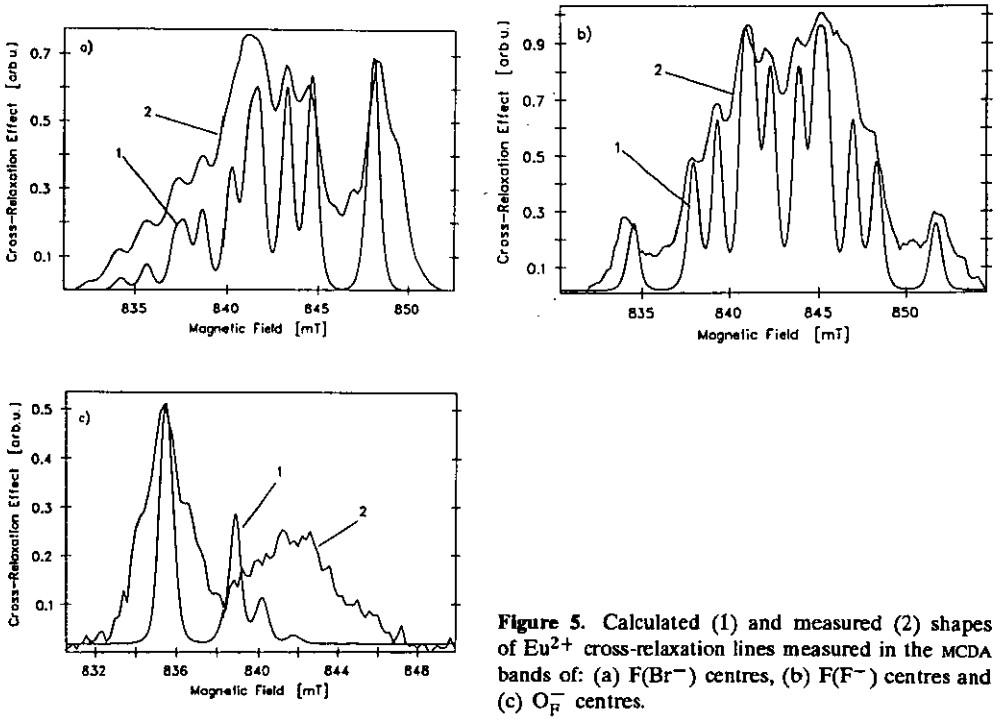

Figure 5. Calculated (1) and measured (2) shapes of Eu^{2+} cross-relaxation lines measured in the MCDA bands of: (a) $F(Br^-)$ centres, (b) $F(F^-)$ centres and (c) O_F^- centres.

The shape of the Eu^{2+} cross-relaxation lines is of a complicated structure. Figures 5(a–c) show this for Eu cross-relaxation lines measured in the MCDA of $F(Br^-)$, $F(F^-)$ and O_F^- centres. The origin of the structured line shape is explained in section 4.2.

4. Discussion of the cross-relaxation effects

4.1. Cross-relaxation mechanism with Eu^{2+}

The shortening of the T_1 times with increasing Eu^{2+} concentration shows that the ground-state polarization of the F and O_F^- centres is coupled to the Eu^{2+} spin system

by cross-relaxation by which the ODEPR effect of Eu^{2+} can be transferred to those centres. For all defects that have a longer T_1 time than the Eu^{2+} spin system a second relaxation channel opens to Eu^{2+} which increases in efficiency as the Eu^{2+} concentration increases. Therefore the decay times of the ODEPR lines of those defects shorten with the Eu^{2+} concentration.

In order for cross-relaxation between two paramagnetic defects to occur, the overlap integral of the shape function of the EPR lines of the two defects must not disappear. The probability of a cross-relaxation process between a $S = 1/2$ system and a $S = 7/2$ system assuming a dipole–dipole interaction is (Bloembergen *et al* 1959):

$$R_{ij} = \hbar^{-2}|H_{ij}|^2 g_{\alpha\beta} \tag{1}$$

with

$$|H_{ij}|^2 = g_i^2 g_j^2 \beta^4 \frac{(1 - 3\cos^2\theta_{ij})^2}{r_{ij}^6} \qquad g_{\alpha\beta} = \int g_\alpha(\nu') g_\beta(\nu')\,\mathrm{d}\nu'$$

$g_{\alpha\beta}$ is the overlap integral of the shape functions of the EPR lines of both defect types α and β. The indices i and j characterize the individual defects of each type taking part in the cross-relaxation and having a distance r_{ij} and angle θ_{ij} between the connection line and the magnetic field. β is the gyromagnetic ratio in the CGS system and g_i, g_j are the g factors.

If we consider the cross-relaxation between Eu^{2+} and the F or O_F^- centres, only the ($m_S = -\frac{1}{2} \rightarrow m_S = +\frac{1}{2}$) transition within the Eu^{2+} spin system has a contribution to the overlap integral for the orientation $\boldsymbol{B} \parallel c$ with the $S = 1/2$ defects with which cross-relaxation to Eu^{2+} takes place. Figure 5 shows the $S = 1/2$ coupling of a defect such as an F centre with the $S = 7/2$ system of Eu^{2+} schematically. The two middle levels ($m_S = -\frac{1}{2}$ and $m_S = +\frac{1}{2}$) of Eu^{2+} are coupled to the F centre. Thus only the spin occupancy of these two levels is important for the cross-relaxation. If an ODEPR transition is excited in the Eu^{2+} spin system, then the two $m_S = \pm\frac{1}{2}$ Eu^{2+} levels are influenced either indirectly or directly in the case of the Eu^{2+} ODEPR transition from $m_S = -\frac{1}{2}$ to $m_S = +\frac{1}{2}$. The change in the occupancy of these two Eu^{2+} spin levels is transferred to the Zeeman levels of the F centre by cross-relaxation. Since the occupancy ratio of the two middle Eu^{2+} Zeeman levels is thus responsible for the sign of the Eu^{2+} cross-relaxation lines in the $F(Br^-)$ ODEPR spectrum, there is a different sign in the spectrum of figure 2(b), curve 1, than when the Eu^{2+} ODEPR is measured directly via the Eu^{2+} MCDA (figure 2(a)) in which the sign of the Eu^{2+} ODEPR depends on the behaviour of the overall Eu^{2+} ground-state polarization.

Cross-relaxation is especially efficient if the cross-relaxation time R_{ij}^{-1} is of the order of the F centre T_1 time or smaller. The influence of cross-relaxation on the decay behaviour of the F centre ODEPR is increased by a short relaxation time (high relaxation rate) within the Eu^{2+} spin system in comparison to the F-centre relaxation time because then the second relaxation channel of the F-centre spin via cross-relaxation to Eu^{2+} becomes more effective. However, it is more favourable for the transfer of the Eu^{2+} ODEPR effect by cross-relaxation if the relaxation rate of the Eu^{2+} spin system is small in comparison with the ODEPR transition rate. Then an ODEPR transition within the Eu^{2+} spin system moves it far away from thermal equilibrium

and thus the spin occupancy of the middle level is influenced greatly by the ODEPR transition. The T_1 time of the Eu^{2+} spin system is much smaller than the T_1 times of the radiation-induced defects ($F(Br^-)$, $F(F^-)$, O_F^- and $Br_2^- - V_K$). Therefore the cross-relaxation channel via the Eu^{2+} spin system is very efficient if the cross-relaxation rate is not the bottle neck. Because of this we could measure a strong decrease in spin lattice relaxation times of the radiation-induced defects with increasing Eu^{2+} doping level. On the other hand, it is easily possible to drive the Eu^{2+} spin system from thermal equilibrium by ODEPR transitions because the relaxation time of the Eu^{2+} is long enough ($T_1 = 0.3$ s at 1.5 K) so that the stationary cross-relaxation effect between Eu^{2+} and for example $F(Br^-)$ can be observed with ODEPR.

In the following we will derive the rate equations which describe the Eu^{2+} spin system and an $S = 1/2$ half system and which will take into account cross-relaxation between these systems. For the sake of simplicity we limit ourselves initially to cross-relaxing defects consisting of one F centre and one Eu^{2+} centre which interact with each other with a certain cross-relaxation probability. This means according to equation (1) that there is a population consisting of F centres and Eu^{2+} ions with a special distance between each other. The cross-relaxation probabilities for a spin flip at the F centre or the Eu^{2+} centre ($R_{F,-\frac{1}{2}\to+\frac{1}{2}/+\frac{1}{2}\to-\frac{1}{2}}$ or $R_{Eu,-\frac{1}{2}\to+\frac{1}{2}/+\frac{1}{2}\to-\frac{1}{2}}$) can be written as follows:

$$\begin{aligned} R_{F,+\frac{1}{2}\to-\frac{1}{2}} &= n_4 R \qquad R_{F,-\frac{1}{2}\to+\frac{1}{2}} = n_5 R \\ R_{Eu,+\frac{1}{2}\to-\frac{1}{2}} &= m_1 R \qquad R_{Eu,-\frac{1}{2}\to+\frac{1}{2}} = m_2 R \end{aligned} \tag{2}$$

where R is the cross-relaxation probability and n_4, n_5, m_1, m_2 are the occupancy numbers of the Eu^{2+} and F centre $m_S = \pm\frac{1}{2}$ states, respectively (see figure 6). R is equal for the two processes, namely spin-up for the F centre and spin-down for the Eu^{2+} centre and vice versa, as can be calculated according to equation (1). If the rate equation for an F centre (or for an O_F^- centre) is formulated taking into account cross-relaxation, one obtains:

$$dm_1/dt = -m_1 R n_5 - m_1 w_{12}^F + m_2 P^F + m_2 w_{21}^F + m_2 R n_4 \tag{3}$$

where P^F is the ODEPR transition probability and w_{12}^F and w_{21}^F are the F-centre relaxation rates between the levels m_1 and m_2 (see figure 6). With the following standardization condition for the total occupancy of the F centres

$$m_1 + m_2 = 1 \tag{4}$$

the rate equation can be expressed only with the occupancy m_1

$$dm_1/dt = -[R(n_4 + n_5) + 2P^F + w_{12}^F + w_{21}^F]m_1 + P^F + w_{21}^F + Rn_4. \tag{5}$$

In Koschnick *et al* (1992c), the rate equations for the Eu^{2+} defect were derived and the relaxation parameters calculated by fitting the equations to the stationary ODEPR spectrum with its anomalous sign changes and to time-resolved dynamical ODEPR experiments. It is shown there that an anomalous spin–lattice relaxation connecting $\Delta m_S = \pm 2$ levels faster then those separated by $\Delta m_S = \pm 1$ operates in this spin

system. If the cross-relaxation rates are included into the Eu^{2+} rate equation system then the equations can be written as follows:

$$\begin{aligned}
dn_1/dt &= [-w_{12} - P_{12} - w_{13} - P_{13}]n_1 + [w_{21} + P_{21}]n_2 + [w_{31} + P_{31}]n_3 \\
dn_2/dt &= [w_{12} + P_{12}]n_1 + [-w_{23} - w_{21} - P_{21} - P_{23} - w_{24} - P_{24}]n_2 \\
&\quad + [w_{32} + P_{32}]n_3 + [w_{42} + P_{42}]n_4 \\
dn_3/dt &= [w_{13} + P_{13}]n_1 + [w_{23} + P_{23}]n_2 + [-w_{34} - w_{32} - P_{34} - P_{32} - w_{31} - w_{35} \\
&\quad - P_{31} - P_{35}]n_3 + [w_{43} + P_{43}]n_4 + [w_{53} + P_{53}]n_5 \\
dn_4/dt &= [w_{24} + P_{24}]n_2 + [w_{34} + P_{34}]n_3 + [-w_{45} - w_{43} - P_{43} - P_{45} - w_{42} - w_{46} \\
&\quad - P_{42} - P_{46} - (1 - m_1)R]n_4 + [w_{54} + P_{54} + m_1 R]n_5 + [w_{64} + P_{64}]n_6 \\
dn_5/dt &= [w_{35} + P_{35}]n_3 + [w_{45} + P_{45} + (1 - m_1)R]n_4 + [-w_{56} - w_{54} - P_{54} - P_{56} \\
&\quad - w_{53} - w_{57} - P_{53} - P_{57} - m_1 R]n_5 + [w_{65} + P_{65}]n_6 + [w_{75} + P_{75}]n_7 \\
dn_6/dt &= [w_{46} + P_{46}]n_4 + [w_{56} + P_{56}]n_5 + [-w_{67} - w_{65} - P_{65} - P_{67} - w_{64} - w_{68} \\
&\quad - P_{64} - P_{68}]n_6 + [w_{76} + P_{76}]n_7 + [w_{86} + P_{86}]n_8 \\
dn_7/dt &= [w_{57} + P_{57}]n_5 + [w_{67} + P_{67}]n_6 + [-w_{78} - w_{76} - P_{76} - P_{78} - w_{75} - P_{75}]n_7 \\
&\quad + [w_{87} + P_{87}]n_8 \\
dn_8/dt &= [w_{68} + P_{68}]n_6 + [w_{78} + P_{78}]n_7 + [-w_{87} - P_{87} - w_{86} - P_{86}]n_8. \qquad (6)
\end{aligned}$$

The F-centre relaxations w_{12}^{F} and w_{21}^{F} can easily be determined from the T_1 time of the F centre because the following holds for a $S = 1/2$ system:

$$T_1 = 1/(w_{12} + w_{21}) \qquad w_{12} = w_{21} \exp(-\Delta E_{12}/kT). \qquad (7)$$

This differential equation system is a non-linear system which contains products of the occupancy of the F centre and the Eu^{2+} defect—for example $m_1(t)Rn_5(t)$. Only the steady-state solution of the differential equation system will be evaluated below. If the time derivatives of the spin occupations are set to zero in order to calculate the steady-state solution, a non-linear equation system is obtained. This equation system can be solved by an iterative method. With an initial value for m_1 (F-centre spin occupation number), the Eu^{2+} spin occupancy (n_i) is determined first. Then the occupancy m_1 for the F centre is calculated with the values n_4 and n_5. The m_1 value is then inserted into the equation system of the Eu^{2+} spin system again. This method converges so rapidly that three iterations are sufficient to obtain a simulation of the cross-relaxation ODEPR spectrum which remains stable. The result of the calculation for cross-relaxation between the $F(Br^-)$ centre and the Eu^{2+} centre is shown in figure 2(b), curve 2. The only free parameter in the computation is the cross-relaxation probability R, since the two values needed for the relaxations of the Eu^{2+} spin system w connecting $\Delta m_S = \pm 2$ and w' connecting $\Delta m_S = \pm 1$ were determined in Koschnick *et al* 1992c ($w = 0.7\ s^{-1}$, $w' = 10\ s^{-1}$). The F-centre relaxations and the O_F^- relaxation are determined by the measured T_1 times.

R was taken to be $0.1\ s^{-1}$, the EPR line shape to be rectangular for simplicity of calculation. This model calculation reproduces the experimental results very well. What is neglected so far is the as yet unknown distribution of F centres in Eu^{2+} ions and the corresponding distribution of R values. This will be discussed in section 4.3.

The cross-relaxation opens a second relaxation channel for the electron spins of the $F(Br^-)$, $F(F^-)$ and the O_F^- centres. If we assume a simple shunt model for the relaxation rates for an F centre, for example, the effective T_1 time becomes:

$$1/T_{1,\text{eff}} = 1/T_{1,F} + 1/(T_{1,Eu} + R^{-1}) \tag{8}$$

If the cross-relaxation probability is very large, the term R^{-1} in equation (10) can be neglected. If, furthermore, the spin–lattice relaxation of the Eu^{2+} spin system is faster than that of the F centre, the effective relaxation time $T_{1,\text{eff}}$ of the F centre is governed by the Eu^{2+} spin–lattice relaxation time $T_{1,Eu}$. This was observed in BaFBr crystals which were doped with 70 ppm Eu^{2+}. Upon variation of the doping level between zero and 70 ppm, the measured relaxation times of the $F(Br^-)$ centre were in the range between the normal T_1 time of about 10 s and the Eu^{2+} T_1 time of about 0.3 s (at 1.5 K). Qualitatively the same was measured for the $F(F^-)$ and the O_F^- centres.

4.2. Cross-relaxation line shape

It will be shown now that the Eu^{2+} fine structure line shape and the line shape, for example, of an F centre influences the shape of the cross-relaxation lines. Eu has two isotopes, each of which has a nuclear spin of $I = \frac{5}{2}$, so each individual fine structure line of Eu^{2+} is split into 12 hyperfine (HF) lines. The HF splitting is not seen in figure 2 because the saturation broadening of the lines due to high microwave power, which also shows up in the observation of the forbidden Eu^{2+} lines ($\Delta m_S = \pm 2$). The nuclear spin of Eu^{2+} can relax first by means of a forbidden transition simultaneously with the electron spin and secondly by phonon-modulated interaction with the neighbouring nuclear spins. As a rule, however, the relaxation rate is much lower than that of the electron spins. Assuming a longer T_1 time of the Eu nuclear spin than the T_1 time of the electron spins, the shape of the cross-relaxation lines can be explained. It then follows that the relaxation time of the Eu^{2+} nuclear spin is also longer than the cross-relaxation time to the F centres or the O_F^- centres, if the cross-relaxation is efficient enough to be observed in the ODEPR spectra. In other words, when an ODEPR transition is excited at Eu^{2+} and is manifested by cross-relaxation in the MCDA of another centre, the nuclear spin of the Eu^{2+} does not change its state during the cross-relaxation process. Thus the cross-relaxation line as observed, for example, in the $F(Br^-)$ ODEPR is an image of the overlap of the HF split ODEPR line of the Eu^{2+} defect and that of the $F(Br^-)$ centre. The area under an Eu^{2+} cross-relaxation line is thus proportional to the overlap integral between the line shape of $F(Br^-)$ and the middle lines ($m_S = \frac{1}{2} \rightarrow -\frac{1}{2}$) of Eu^{2+}(see equation (1)). Thus the line shape given by the derivative of the overlap integral of the ODEPR shape functions of the cross-relaxing defects with respect to the magnetic field. The line shape of the F centres and the O_F^- centres is determined by inhomogeneous broadening because of unresolved ligand HF interactions, while the EPR line of the Eu^{2+} ions is split by the Eu^{2+} HF interaction of each isotope. The HF interactions are small compared to the electron Zeeman term, and can be taken into account in first order. Thus the frequency of the microwave field ν has a linear dependence on the magnetic field B:

$$h\nu = \mu_B g B + \sum_i a_i m_I.$$

It follows that

$$d\nu/dB = \mu_B g/h \tag{9}$$

therefore, the integration variable ν of the overlap integral in equation (1) can easily be transformed to the magnetic field B

$$\int g_\alpha(\nu)g_\beta(\nu)\,d\nu = \frac{\mu_B g}{h}\int g_\alpha(B)g_\beta(B)\,dB. \tag{10}$$

It follows that

$$\frac{d}{dB}\left(\int g_\alpha(\nu)g_\beta(\nu)\,d\nu\right) = \frac{\mu_B g}{h}\frac{d}{dB}\left(\int g_\alpha(B)g_\beta(B)\,dB\right) \propto g_\alpha(B)g_\beta(B). \tag{11}$$

The shape of the Eu^{2+} cross-relaxation $m_S = 1/2 \rightarrow m_S = -1/2$ lines is thus given by the product of the ODEPR shape functions of the Eu^{2+} line, which is split by the HF interaction, multiplied by the ODEPR shape function of one of both F-centre types or the O_F^- centre. Figures 5(a–c) show the Eu^{2+} cross-relaxation lines measured via the MCDA of the three defects $F(Br^-)$, $F(F^-)$, O_F^- centres (curve 2) compared to a calculation according to equation (13) (curve 1). The agreement is excellent in the case of F centres. With the O_F^- centre, at least a qualitative description of the line shape was achieved. For the calculation of the cross-relaxation line shape the EPR lineshape of the Eu^{2+} $m_S = 1/2 \rightarrow -1/2$ transition was taken from conventional EPR measurements because the ODEPR line shape is always saturation-broadened and less well resolved. The cross-relaxation lines are also saturation-broadened which was not included in the calculation. The shape of the cross-relaxation lines was found to be independent of the microwave power except for saturation-broadening effects.

In the cross-relaxation spectra measured in the MCDA of the Br_2^-–V_K centre with the cross relaxation lines of the $F(Br^-)$ and the Eu^{2+} centres (see figure 3(c)) the shape of the Eu^{2+} cross-relaxation lines is the same as that of the Eu^{2+}–$F(Br^-)$ cross-relaxation measured in the $F(Br^-)$ MCDA. Thus the line shape cannot be explained by the overlap of the Br_2^-–V_K ODEPR with the Eu^{2+} fine structure line ($m_S = \frac{1}{2} \rightarrow m_S = \frac{3}{2}$). The Eu^{2+} cross-relaxation is transferred indirectly via the $F(Br^-)$ centre to the Br_2^-–V_K centre. Cross-relaxation effects between the Br_2^-–V_K centres and the $F(Br^-)$ centres were already observed in undoped BaFBr and reported in Koschnick *et al* 1992b.

4.3. Calculation of the cross-relaxation effect for a statistical defect distribution

According to equation (1), the cross-relaxation probability R depends on the distance between the cross-relaxing defects as well as on the angle with respect to the magnetic field of the connection vector between the two defects. In the calculation of the ODEPR spectrum of the $F(Br^-)$ centre with the Eu^{2+} cross-relaxation of figure 2, curve 1, only one cross-relaxation probability R was assumed, i.e. the calculation was performed with an ensemble consisting of only one cross-relaxation system with a certain spacing and angle. However, there is a three-dimensional distribution of Eu^{2+}, $F(Br^-)$, $F(F^-)$ and O_F^- centres in the crystal. The cross-relaxation effect measured via the MCDA of the $F(Br^-)$ centres, for example, consists of a sum of many cross-relaxations R_{ij} of different strengths. In the following we show that a purely random

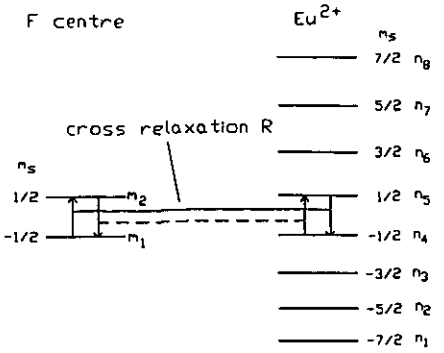

Figure 6. Schematic diagram of the cross-relaxation of the Eu^{2+} spin system with an F centre. The two middle Eu^{2+} Zeeman levels are in resonance with the two Zeeman levels of the F centre. m_i, n_j are the occupancy numbers of the F and Eu^{2+} levels, respectively.

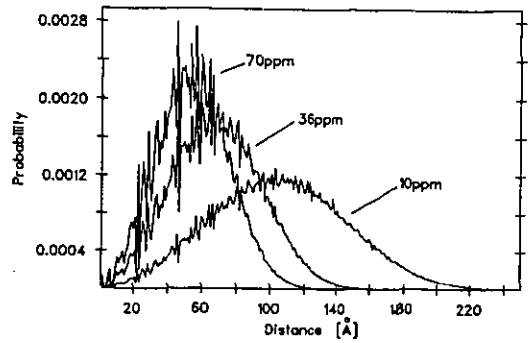

Figure 7. Probability distribution of the Eu^{2+}–$F(Br^-)$ distances in BaFBr with a purely random defect distribution and various Eu^{2+} concentrations. The 'structures' superimposed on the distributions are caused by discrete lattice distances and by the lattice structure.

distribution of defects cannot explain the measured cross-relaxation effects. First we calculated the cross-relaxation effects with the assumption of a random distribution between e.g. the radiation-produced $F(Br^-)$ centres and the Eu^{2+} activator.

The concentration of the $F(Br^-)$ defects was 10^{16} cm^{-3} and thus much smaller than the Eu^{2+} concentration; it can be assumed that the $F(Br^-)$ centres do not interact with each other. From this follows that the BaFBr crystal can be subdivided into blocks with one $F(Br^-)$ centre in each block. These blocks then form the statistical population. Within a block, all possible Eu^{2+} lattice sites (i.e. the Ba^{2+} sites) in the vicinity of the $F(Br^-)$ centres are determined with the help of a cumputer program and then distance and angular distributions are calculated. The distance distribution indicates the number of possible Eu^{2+} sites as a function of the distance from the $F(Br^-)$ centre. The angular distribution indicates how many of these sites at a certain distance from the $F(Br^-)$ have a connecting vector to the $F(Br^-)$ centre at a certain angle with respect to the magnetic field. Whether a Ba^{2+} site will be occupied by an Eu^{2+} or not can be represented by a binomial distribution that develops into a Poisson distribution at low probabilities. The $F(Br^-)$–Eu^{2+} distance distribution is calculated as the probability that one or more Eu^{2+} defects are present in a spherical shell of radius r_{ij} from the $F(Br^-)$ centre, where there are a certain number of Ba^{2+} sites. Within this spherical shell, various angular ranges are also differentiated. This is performed for all spacings and angles within the selected $F(Br^-)$ centre environment with the help of a program that takes into account the lattice geometry of the crystal. If a $F(Br^-)$ centre with several Eu^{2+} defects enters into an interaction within the selected environment, then only the interaction that takes place with the Eu^{2+} defect that has the smaller distance from the $F(Br^-)$ centre is important because the distance enters the cross-relaxation equation with r_{ij}^{-6}. It follows from this that only Eu^{2+}–$F(Br^-)$ pairs need be considered. The probability $W_1(r_{ij}, \theta_{ij})$ that an Eu^{2+} defect with an angle θ_{ij} of the connection vector to the $F(Br^-)$ centre will occur in a shell at a distance r_{ij} from the $F(Br^-)$ centre must also be multiplied by the probability $W_0(r_{ij})$ of there being no Eu^{2+} defect within the sphere of radius r_{ij}. This yields

the probability $W(r_{ij}, \theta_{ij})$, which indicates the probability of there being exactly one Eu^{2+} defect at a distance r_{ij} and an angle θ_{ij} relative to the $F(Br^-)$ centre and no Eu^{2+} defect at a smaller distance from the $F(Br^-)$ centre:

$$W(r_{ij}, \theta_{ij}) = W_1(r_{ij}, \theta_{ij}) W_0(r_{ij}). \tag{12}$$

The probabilities W_1 and W_0 are calculated according to the Poisson distribution

$$W_1(r_{ij}, \theta_{ij}) = \overline{n}_1 \exp(-\overline{n}_1) \qquad W_0(r_{ij}) = \exp(-\overline{n}_0) \tag{13}$$

where

$$\overline{n}_1 = [\mathrm{Eu}] P_{\mathrm{Eu}}(r_{ij}, \theta_{ij}) \qquad \overline{n}_0 = [\mathrm{Eu}] P_{\mathrm{Eu}}(< r_{ij}). \tag{14}$$

[Eu] is the Eu^{2+} concentration. $P_{\mathrm{Eu}}(r_{ij}, \theta_{ij})$ is the number of possible Eu^{2+} sites at a distance r_{ij} and angle θ_{ij}. $P_{\mathrm{Eu}}(< r_{ij})$ is the number of possible Eu^{2+} sites within the sphere with a radius r_{ij}. Figure 7 shows the probability of the existance of Eu^{2+}–$F(Br^-)$ pairs at a distance in Å for the various Eu^{2+} concentrations used in the experiments. The distribution was calculated in 1Å increments from a minimum distance of 2 Å up to 400 Å from the $F(Br^-)$ centre. Within this probability distribution, $F(Br^-)$–Eu^{2+}–Eu^{2+} triples were also included, where the two Eu^{2+} defects are at the same distance from the $F(Br^-)$ centre. Higher combinations can be disregarded.

For the individual angles and for the various distances, the cross-relaxation probability R_{ij} and thus the cross-relaxation ODEPR spectrum can now be calculated. The spectrum measured in the experiment is the sum of all individual cross-relaxation ODEPR spectra. Thus in the simulation for each calculated distance and angle, the cross-relaxation spectrum was calculated, weighted with the probability for this constellation and then all contributions were summed. Figure 8 shows the results of the simulation of the Eu^{2+}–$F(Br^-)$ cross-relaxation with a random defect distribution for an Eu^{2+} concentration of 10 ppm. The calculated cross-relaxation effect is much too small compared to the measured effect shown in figure 2(b), curve 1. For the O_F^- centre, the result is even less adequate because the O_F^- centre has a shorter T_1 time and a smaller overlap with the Eu^{2+} ODEPR than the $F(Br^-)$ centre and thus the cross-relaxation effect is smaller.

The calculations show that a purely random distribution of the defects cannot explain the cross-relaxation observations. There must be a spatial correlation of the F centres and the O_F^- centres with the Eu^{2+} defects. In addition, the calculations show that the Br_2^-–V_K centre must have a correlation with the $F(Br^-)$ centre and the Eu^{2+} centre.

The actual distribution of the defects in the crystal cannot be determined unambiguously from the cross-relaxation spectra. The cross-relaxation spectroscopy and the quantitative analysis could only show that there cannot be a random distribution between the paramagnetic defects, but it is difficult to estimate the relative amount of defects which are correlated and the distance between them. The number of relevant cross-relaxing defects as well as the distance which determines the efficiency of cross-relaxation, are free parameters in the calculation if one deviates from a purely random distribution.

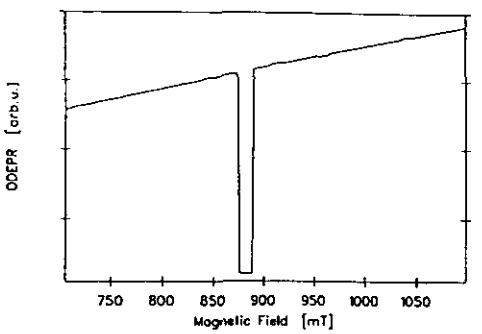

Figure 8. Calculation of the ODEPR spectra and cross-relaxation effects obtained in the MCDA of $F(Br^-)$ centres in BaFBr doped with 10 ppm Eu^{2+} assuming a purely statistical distribution of $F(Br^-)$ centres (10^{16} cm^{-3}) and Eu^{2+} (T = 1.5 K). Almost no cross-relaxation effect is obtained with the assumption of a random defect distribution.

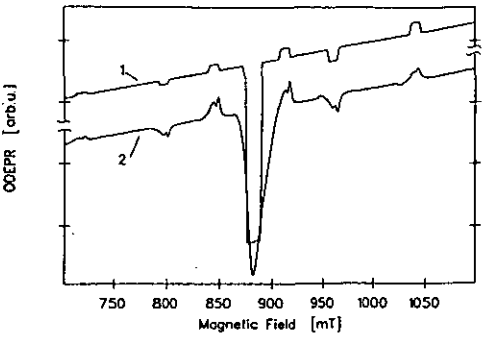

Figure 9. Cross-relaxation effect in the MCDA of the $F(Br^-)$ centre at an Eu^{2+} concentration of 10 ppm and at T = 1.5 K. Curve 1: calculated with the assumption that 10% $F(Br^-)$ centres are correlated to Eu^{2+} centres with a cross-relaxation distance of about 20 Å, 10 ppm Eu^{2+} 10^{16} cm^{-3} F centres (see text). Curve 2: measured effect at T = 1.5 K in BaFBr doped with 10 ppm Eu^{2+} containing 10^{16} cm^{-3} F centres.

If it is assumed that with an Eu^{2+} concentration of 10 ppm, some of the F centres are a distance between 15 and 20 Å away from the Eu^{2+} ion (which is the minimum distance required because no line splittings due to spin–spin interactions were observed), then the experimental cross-relaxation effects can be explained if 10% of the F centres are correlated to the Eu^{2+} at this distance and the rest of 90% are randomly distributed (figure 9). For an Eu^{2+} concentration of 70 ppm, similar calculations show that about 50% of the F centres are correlated within a distance between 15 and 20 Å. Thus cross-relaxation measurements and calculations have shown that at least a fraction of the radiation defects must be spatially correlated to the Eu^{2+} ions. But this correlation must have an intermediate character. This means that a nearest-neighbour relation to the Eu^{2+} ions can be ruled out because then an additional splitting of the ODEPR by the strong spin–spin interaction would have been observed. Also it may be that there is a distribution of different correlations. It is strange to have to assume that defects have a spatial correlation with a distance which is larger than two lattice distances (15 Å) but small enough to have cross-relaxations. In this stage of the investigation, one can only speculate about the reasons for the spatial correlation. Perhaps the layer structure of the crystal lattice of BaFBr is responsible for these correlations. Also an exciton decay mechanism into radiation defects in the neighbourhood of an Eu^{2+} ion which is smaller than Ba^{2+} and thus causes a lattice relaxation may cause those spatial correlations.

5. Conclusions

In x-irradiated Eu^{2+}-doped BaFBr, the radiation defects have spin–spin interactions with the Eu^{2+} activator ions via cross-relaxation. The analysis of the cross-relaxation effects as a function of the Eu^{2+}doping level showed that a random distribution

between the radiation defects and the Eu^{2+} ions does not exist. A fraction of the radiation defects which cannot be neglected must have a spatial correlation to the Eu^{2+} defects as well as the V_K and $F(Br^-)$ centres produced at low temperature by x-irradiation, giving important clues about their production mechanism (for details see Koschnick *et al* 1991, 1992a,b).

Our experiment and analysis represent a first step towards cross-relaxation spectroscopy by which spatial correlations between paramagnetic defects can be discovered. This is particularly useful if the distances between the defects remain large such that direct interactions cannot be resolved in the spectra.

As for the storage phosphor $BaFBr:Eu^{2+}$ our experiments provide the first direct experimental evidence for a spatial correlation between the defects involved in the PSL process. Possibly this is one of the reasons why this storage phosphor is one of the most successful ones.

References

Ahlers F J, Lohse F, Spaeth J-M, and Mollenauer L F 1983 *Phys. Rev.* B **28** 1249

Bloembergen N, Shapiro S, Pershan P S and Artman J O 1959 *Phys. Rev.* **114** 445

Brixner L H, Bierlein J D and Johnson V 1980 *Eu^{2+} Fluorescence and its Application in Medical x-ray Intensifying Screens (Current Topics in Material Science 4)* (Amsterdam: North-Holland) p 47

Eachus R S, McDugle W G, Nuttall R H D, Olm M T, Koschnick F K, Hangleiter Th and Spaeth J-M 1991a *J. Phys.: Condens. Matter* **3** 9327

—— 1991b *J. Phys.: Condens. Matter* **3** 9339

Geschwind S 1972 *Electron Paramagnetic Resonance* ed S Geschwind (New York: Plenum) p 233

Hangleiter Th, Koschnick F K, Spaeth J-M and Eachus R S 1990 *J. Phys.: Condens. Matter* **2** 6837

Koschnick F K, Hangleiter Th, Spaeth J-M and Eachus R S 1992a *J. Phys.: Condens. Matter* **4** 3001

Koschnick F K, Spaeth J-M and Eachus R S 1992b *J. Phys.: Condens. Matter* **4** 3015

—— 1992c *J. Phys.: Condens. Matter* submitted

Koschnick F K, Spaeth J-M, Eachus R S, McDugle W G and Nuttall R H D 1991 *Phys. Rev. Lett.* **67** 3571

Luckey G W 1975 *US Patent 3,859,527,1983*. Revised 31847

Seggern von H, Voigt T, Knüpfer W and Lange G 1988 *J. Appl. Phys.* **64** 1405

Stevels A L N and Pingault F 1975 *Philips Res. Rep.* **30** 277

Takahashi K, Miyahara J and Shibahara J 1985 *J. Electrochem. Soc.* **312** 1492